Searching for Signs of a Galactic Excess of Gravitational Waves

Serena Moseley and Thomas Callister

California Institute of Technology

(Dated: August 3, 2018)

I. INTRODUCTION

A. Gravitational Wave Astronomy

General relativity predicts the existence of gravitational waves, oscillations in the space-time metric that are produced by massive, accelerating objects. Since 2015, gravitational waves have been routinely detected by the Advanced LIGO [1] and Advanced Virgo [2] experiments. Compact binary coalescences (CBCs), namely binary black hole mergers and binary neutron star mergers, have been responsible for all of the gravitational-wave signals detected so far. Signals from CBCs have peak amplitudes at frequencies within the most sensitive band of the Advanced LIGO detectors, between approximately 100 and 1000 Hz [3]. This and the fact that compact binary objects merge at a fairly high rate in the local Universe together make these events the only gravitational-wave sources observed to date.

Besides signals from CBC mergers, the LIGO and Virgo collaborations (LSC/Virgo) also search for a variety of other kinds of signals, including continuous gravitational waves, stochastic gravitational waves, and burst gravitational waves. These searches may be grouped into one of two categories: either modeled or unmodeled searches, depending on the signal of interest. In modeled searches, such as those for CBCs, we can predict deterministically what the gravitational-wave signal should look like in the data. We can create template waveforms spanning the space of possible CBC signals and search through the data for a match. We perform this matched filter to reduce various noise that can drown out the signal and to boost the signal-to-noise ratio [4]. In contrast, other gravitational-wave signals involve so many unknowns that we cannot know beforehand what they may look like in the data. For this reason, LSC/Virgo also conduct unmodeled searches that don't rely on strong a priori assumptions about the form of the signal. Burst searches are generally unmodeled searches for signals from an unknown transient event. Examples of events that

produce gravitational-wave bursts include supernovae and glitching neutron stars, in which a spinning neutron star suddenly changes its spin period [5]. For this project, we will broadly work within the realm of burst searches.

B. Galactic Excess of Gravitational Waves

In nearly every electromagnetic frequency band, the Milky Way stands out as the brightest source in the sky. Given the recent discoveries of gravitational waves, a new "messenger" of astronomical information, we might expect the galaxy to be a similarly bright source of gravitational radiation in the sky. In fact, we already know that such a galactic excess must exist due to the vast quantity of white dwarf binaries that inhabit the Milky Way [6]. These binaries systems, either resolvable or unresolvable, are a significant source of gravitational radiation in the galaxy [5]. However, although we know galactic white dwarf binaries exist, we cannot detect them with current ground-based detectors. These systems emit gravitational radiation at frequencies that are several orders of magnitude too small to be detected by either Advanced LIGO or Advanced Virgo. This is illustrated in Fig. 1, which graphs the frequency range of the galactic white dwarf population as well as the sensitivity curves of the current ground-based detectors. As the figure demonstrates, we can expect white dwarf binaries to be detectable by the Laser Interferometer Space Antenna (LISA).

While we have yet to identify any galactic excess of gravitational waves in the detectors' output, it may be the case that an unknown galactic source is emitting radiation at frequencies accessible to Advanced LIGO and Advanced Virgo. If such sources do exist, they are likely weak as no associated signals have been clearly detected so far. Even if each burst is too weak to detect individually, we can try to detect their combined population by examining the sky distribution of burst triggers. If a real galactic population exists, we can expect the apparent sky direction of the triggers to align with the galaxy. Otherwise, an isotropic distribution in which the sky direction appears random implies the galactic population does not exist. Separately, it is likely that the detectors will one day discover some previously unknown source population. Once this happens, we will need to be able to identify the source population; knowing the population's distribution on the sky will help to characterize it. Thus we seek to develop a method of mapping the sky distribution of

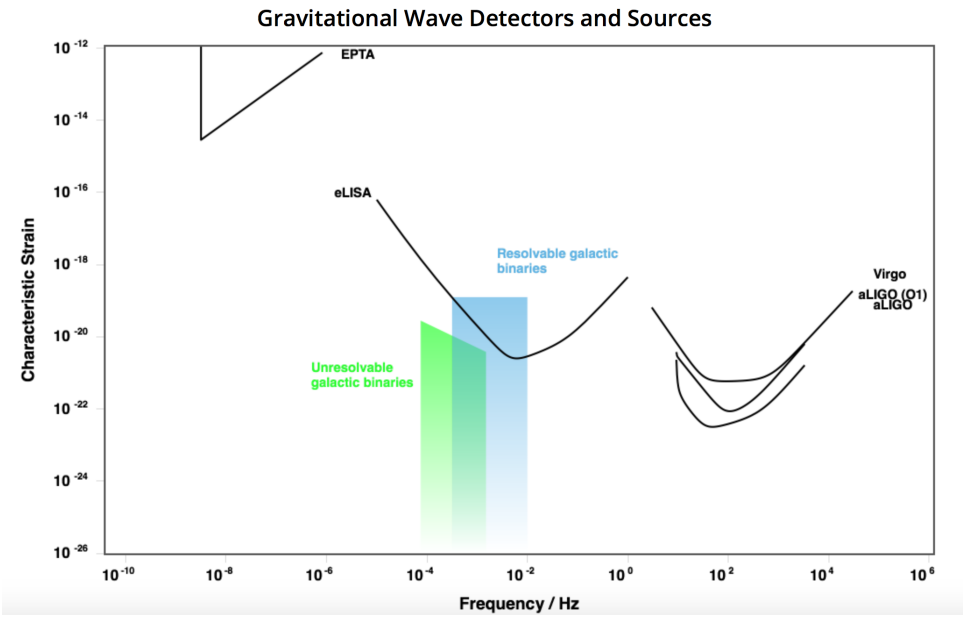

FIG. 1: A plot of the frequency band for unresolvable and resolvable galactic binaries, as well as the sensitivity of Advanced LIGO [7]. The frequency band of the galactic binaries is out of range of the Advanced LIGO sensitivity curve.

unmodeled gravitational-wave bursts to determine whether there exists a galactic excess of gravitational waves in the LIGO-Virgo frequency band.

II. MAPPING WITH BAYESWAVE

A. Skymaps

The localization of a gravitational-wave source depends primarily on two measurements: the difference in arrival times of the signal at the two detectors, and the relative amplitudes measured by each detector. We can use skymaps to map the posterior probability of a signal originating from multiple locations on the sky. Skymaps are two-dimensional projections of the entire sky with colored regions to demonstrate the probability distribution of origin locations for the mapped signal.

When a gravitational wave passes through the Earth and is detected by Advanced LIGO, the time difference between its arrival at the two detectors reveals information about the source location of the signal. For example, if the gravitational-wave signal arrives at both detectors at the same exact time, then the gravitational wave must have traveled along a path perpendicular to the line connecting the two detectors. This constrains the possible

source directions to a single circle on the sky. In Fig. 2, we see an example of a typical gravitational wave skymap. The probability distribution of the signal's source location traces a ring on the sky.

We can partially break the remaining degeneracy by taking the orientations of the two detectors into account. The two Advanced LIGO detectors are oriented slightly different to each other due to the curvature of Earth's surface. These different orientations mean that the detectors are more sensitive to different regions in the sky. If a signal appears louder in one detector than it does in the other, we can say that the signal is more likely to have come from the region it is more sensitive to on the sky.

Skymaps can be created using a mollweide projection, which is a systematic transformation of latitudes and longitudes onto a two dimensional ellipse. This projection is such that the latitude lines are straight and the longitude lines curve as they deviate east or west of the central meridian. This ellipse is divided up into equal-area grid, as seen in Fig. 2.

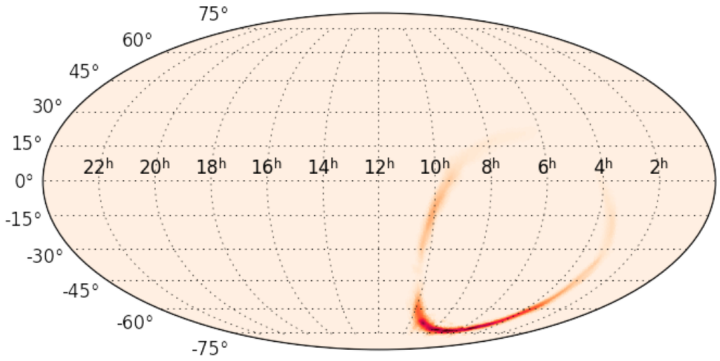

FIG. 2: A mollweide projection skymap, produced by the megasky.py script.

We can compute the gravitational-wave brightness of each pixel on a skymap using HEALPix software. HEALPix minimizes distortion and splits the skymap into equal area pixels of various heights. The heights correspond to the number of events coming from that bin's location on the sky, giving the brightness [8].

B. Bayesian Statistics and Bayeswave

Bayes' Theorem states that the probability of some event A given some event B, known as the posterior probability, is as follows (1):

$$P(A \mid B) = \frac{P(B \mid A)\, P(A)}{P(B)}, \tag{1}$$

where $P(B \mid A)$ is the likelihood, $P(A)$ is the prior probability, and $P(B)$ is the evidence [9]. If we consider some parameter θ and we have a prior probability for it, we can use Baye's Theorem to update the probability of θ given new information. Thus, we can compute the posterior probabilities required for plotting gravitational-wave bursts on skymaps. Rather than compute the probabilities ourselves, we can use Bayeswave to produce posterior samples. Bayeswave is an algorithm that reconstructs gravitational-wave signals using an arbitrary number of Sine-Gaussian wavelets [9]. It generates posterior samples that can be used to estimate model parameters and allows us to reconstruct a gravitational-wave signal without a predicted waveform. In (Fig. 3), we see a Bayeswave-reconstructed strain plot for the gravitational-wave signal from the first binary black hole merger detection, GW150914.

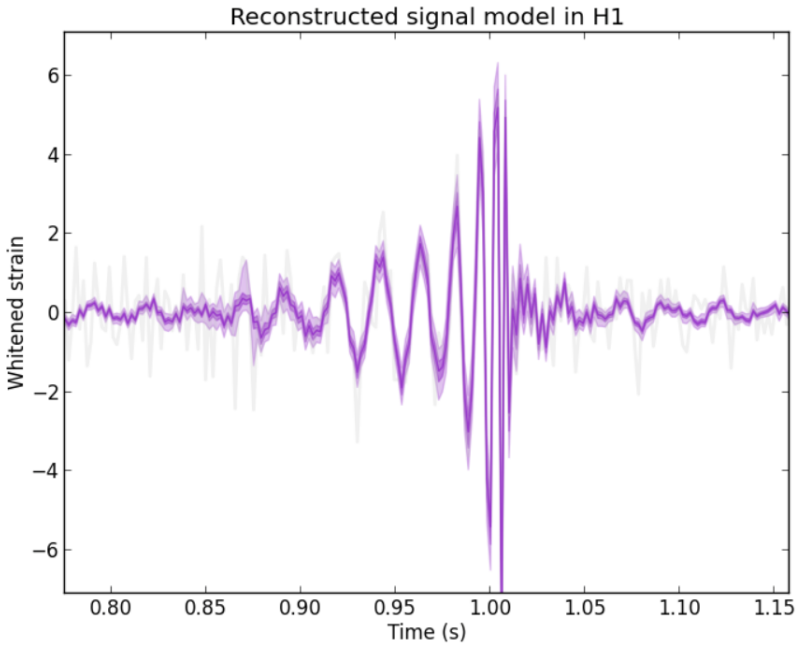

FIG. 3: A reconstructed strain plot for GW150914 generated by the megaplot.py script.

C. Modeling the Galactic Distribution

The Milky Way galaxy appears on our night sky as a long disk of stars, gas, and dust. The structure of this galactic disk can be broken down into two sub-components: a thin and thick disk comprised of two distinct stellar populations. The thin disk encompasses the region of current star formation in the galaxy. It has a smaller volume yet greater density of stars than the thick disk. The thick disk, by comparison, is composed of older stars at a density of about 8.5% the star population density inside of the thin disk [10].

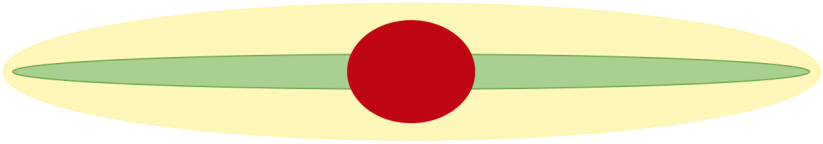

FIG. 4: A diagram of the galactic disk structure. The red circle represents the galactic bulge, while the green and yellow disks represent the thin and thick disks respectively. The scale height of the Milky Way's thin disk is about 350 pc while the scale height of the thick disk is about 1000 pc.

We can model the distribution of stars in the Milky Way galaxy by combining empirical knowledge about the thin and thick disks to generate a stellar number density function (2),

$$n(z,r) = n_0 \left(e^{-z/z_{\text{thin}}} + 0.085e^{-z/z_{\text{thick}}}\right) e^{-r/h_R}, \tag{2}$$

where z is the vertical height above the midplane of the Galaxy, r is the radial distance from the Galactic center, n_0 is the relative density coefficient, z_{thin} is the scale height of the thin disk, z_{thick} is the scale height of the thick disk, and h_R is the disk scale length. This equation is modeled in cylindrical coordinates, however ϕ does not appear in the function because there is no preferred ϕ direction [10].

We will use Eq. (2) to simulate a population of sources distributed randomly throughout the galaxy. We will say that the probability, $p(z,r,\phi)$, of a gravitational wave occuring at the position (z,r,ϕ) is directly proportional to Eq. (2). As the probability must sum to 1 over all space, we can further say that the volume integral of $p(z,r,\phi)$ over all space must equal 1. Combining this with the knowledge that (3)

$$dV = rdrd\phi dz, \tag{3}$$

allows us to derive three normalized, independent probability density functions (PDFs) for each coordinate. Through integration, we can derive their cumulative density function (CDF) counterparts (4), (5), (6):

$$cz(z) = \begin{cases} 1 - z_0(z_{\text{thin}}e^{-z/z_{\text{thin}}} + 0.085z_{\text{thick}}e^{-z/z_{\text{thick}}}) & z > 0 \\ z_0(z_{\text{thin}}e^{z/z_{\text{thin}}} + 0.085z_{\text{thick}}e^{z/z_{\text{thick}}}) & z \leq 0 \end{cases}, \tag{4}$$

$$cr(r) = 1 - \frac{r}{h_R}e^{-r/h_R} - e^{-r/h_R}, \tag{5}$$

$$c\phi(\phi) = \frac{\phi}{2\pi}, \tag{6}$$

where z_0 is the normalization constant for the z-coordinate PDF,

We then invert these three CDFS to obtain z, r, and ϕ as a function of cumulative probability. The CDFs for z and r cannot be readily inverted, so we must generate random samples and interpolate a numerical solution for both. We can convert random c values on the interval (0,1) to random z, r, and ϕ coordinates and plot these coordinates to create a model of the galaxy (Fig. 8). We can also convert from cylindrical to Cartesian, galactic, and ultimately equatorial coordinates. The relationship between galactic (b and l) and equatorial coordinates (α and δ) is as follows (7), (8), (9):

$$\sin(\delta) = \sin(\delta_{NGP})\sin(b) + \cos(\delta_{NGP})\cos(b)\cos(l_{NCP} - l), \tag{7}$$

$$\cos(\delta)\sin(\alpha - \alpha_{NGP}) = \cos(b)\sin(l_{NCP} - l), \tag{8}$$

$$\cos(\delta)\cos(\alpha - \alpha_{NGP}) = \cos(\delta_{NGP})\sin(b) - \sin(\delta_{NGP})\cos(b)\cos(l_{NGP} - l), \tag{9}$$

where NGP refers to the North Galactic Pole and NCP refers to the North Celestial Pole. Equatorial coordinates map directly to right ascension and declination, with α representing right ascension and δ representing declination.

III. OBJECTIVES

We will develop a method to search for signs of excess galactic gravitational waves by generating skymaps from data simulating gravitational-wave bursts. We will inject two large sets of triggers into Bayeswave to obtain posterior samples. One of these sets will represent

an isotropic distribution while the other will be galactically distributed across the sky. We will then use these posterior samples to generate HEALPix bin heights so that we can generate skymaps for our triggers. We aim to use the nested sampling algorithm Multinest to conduct parameter estimation on these HEALPix pixels, and ultimately combine the resultant skymaps for our population of events into a probability distribution of source locations. If a population of galactic gravitational-wave bursts exists within the data, then we would expect to see a galactic disk in this composite probability distribution. If this population does not exist, or if the bursts are isotropic, then we would expect to see a lack of structure within the probability distribution.

IV. PROGRESS ON PROJECT

Our initial proposed timeline was as follows:

Weeks 1-2: Learn how to simulate data and run Bayeswave on it.

Weeks 3-5: Simulate pure signals with no noise and demonstrate that we can recover a map of the galaxy from it.

Weeks 6-7: Simulate pure noise and show that we cannot recover a meaningful map from it.

Weeks 8-10: Put the signals and noise together and recover a galactic plane from it. Do the same with real LIGO data if time allows.

We have successfully written a Python script that takes input right ascension and declination coordinates for many events generated by Bayeswave and plots them on a HEALPix skymap (Fig. 5).

A certain number of initial samples from Bayeswave's burn-in stage are incongruent with the rest of the population and therefore need to be discarded, as seen in the times series for the right ascension and declination coordinates (Fig. 6, 7). Additionally, the set must be downsampled to ensure each sample is independent of each other. We have added the appropriate methods to our code to discard a variable number of initial samples and downsample the data set by its correlation length, computed with Acor.

We have successfully run our first set of injections in Bayeswave. This set consisted of 500 injections isotropically distributed across the sky. They had a Q factor of 5, a frequency

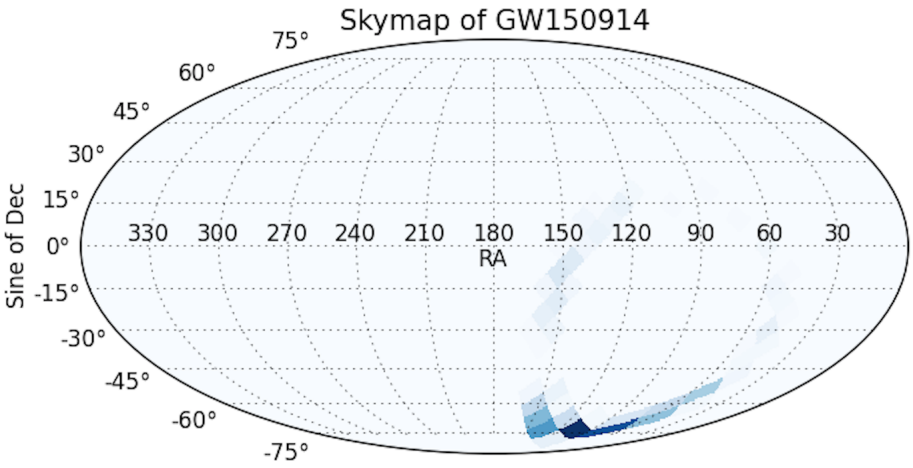

FIG. 5: A HEALPix map for GW150914 generated by our skymap.py script.

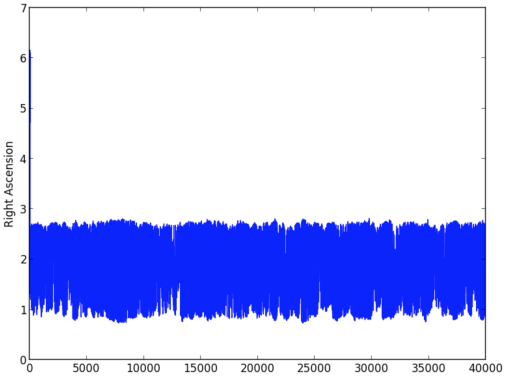

FIG. 6: A plot of the right ascension values for 40,000 samples, created by our skymap.py script. Note the peak in values for the initial samples from the burn-in stage.

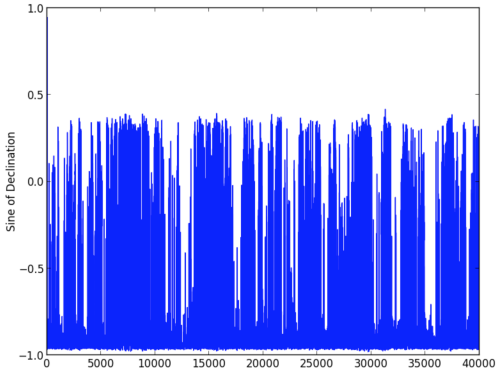

FIG. 7: A plot of the sine of the declination values for 40,000 samples, created by our skymap.py script. Note the peak in values for the initial samples from the burn-in stage.

of 200 Hz, and a maximum strain amplitude of 10^{-22}m. In order to expedite processing of the injection sets, we wrote a script that iterates through each injection in a given set, creates its associated HEALPix map, and stores both the map and the signal evidence for the injection in dictionaries.

We are currently working to create a galactically-distributed injection set. We successfully applied the equations described in the Modeling the Galactic Distribution section to create a model of the distribution of stars in the Milky Way galaxy (Fig. 8). We aim to write code that can convert between coordinate systems and implement this distribution in our code that generates injection sets.

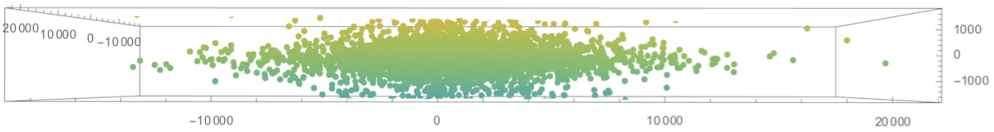

FIG. 8: galactic disk side-view

[1] LIGO Scientific Collaboration, "Advanced LIGO", arXiv:1411.4547, 17 November 2014, DOI: 10.1088/0264-9381/32/7/074001.

[2] F. Acernese, et al. "Advanced Virgo: a 2nd generation interferometric gravitational wave detector", arXiv:1408.3978v3, 16 October 2014, DOI: 10.1088/0264-9381/32/2/024001.

[3] B.P. Abbott et al. (LIGO Scientific Collaboration and Virgo Collaboration), "Observation of Gravitational Waves from a Binary Black Hole Merger", Phys. Rev. Lett., Vol. 116, Iss. 6, (2016).

[4] Alexander Urban, "Signal Processing for GW Astrophysics", LIGO SURF Lecture, 25 June 2018.

[5] B.S. Sathyaprakash and Bernard F. Schutz, Physics, Astrophysics and Cosmology with Gravitational Waves, Living Rev. Relativity, 12, (2009), 2. [Online Article]: http://www.livingreviews.org/lrr-2009-2.

[6] Christopher Moore, et al. Gravitational Wave Detectors and Sources. Gravitational Wave Sensitivity Curve Plotter, Institute of Astronomy, University of Cambridge, rhcole.com/apps/GWplotter/.

[7] Andrzej Krolak, " White Dwarf binaries as gravitational wave sources " in: Einstein Online Band 04 (2010), 1001.

[8] Mark R. Calabretta, Boudewijn F. Roukema; Mapping on the HEALPix grid, Monthly Notices of the Royal Astronomical Society, Volume 381, Issue 2, 21 October 2007, Pages 865872, https://doi.org/10.1111/j.1365-2966.2007.12297.x

[9] J.K. Kruschke, "Bayesian Data Analysis for Newcomers". Psychon Bull Rev, Psychonomic Society, 12 April 2017, DOI 10.3758/s13423-017-1272-1.

[10] Carroll, Bradley W., and Dale A. Ostlie, "An Introduction to Modern Astrophysics". Cambridge University Press, 2017.

[11] Correspondence with Tom Callister